2012

Determining forces required to override obstacles for ground vehicles

George L. Mason
US Army Engineer Research and Development Center, George.L.Mason@us.army.mil

Burhman Q. Gates
US Army Engineer Research and Development Center, Burhman.Gates@us.army.mil

Victoria D. Moore
US Army Engineer Research and Development Center, Victoria.D.Moore@us.army.mil

Available online at www.sciencedirect.com

SciVerse ScienceDirect

Journal of Terramechanics 49 (2012) 191–196

Journal of Terramechanics

www.elsevier.com/locate/jterra

Determining forces required to override obstacles for ground vehicles

George L. Mason *, Burhman Q. Gates, Victoria D. Moore

US Army Engineer Research and Development Center, Geotechnical and Structures Laboratory, United States

Received 29 September 2011; received in revised form 31 January 2012; accepted 17 April 2012
Available online 14 June 2012

Abstract

The military is constantly expanding the use of unmanned ground vehicles in warfighting applications that often involve complex environments. Part of the focus of military research is to improve or validate existing routing algorithms which are used to predict vehicle mobility. Routing algorithms are based on the time required for vehicle movement through a series of obstacles such as trees or fences, thus requiring an assessment of the ability to override such obstacles as compared to finding an alternate maneuver path. The required overriding force can be computed and compared to a vehicle's tractive force to determine the best viable option. If overriding the obstacle is an option (tractive force exceeds the required overriding force), the delay in overriding can be assessed as compared to the delay in maneuvering around the obstacle. This study provides a quick and reasonable calculation of the force required to override specific types of vertically embedded obstacles to support the determination of movement capabilities for unmanned ground vehicles on the battlefield. Published by Elsevier Ltd. on behalf of ISTVS.

Keywords: Obstacle; Force; Velocity; Vegetation; Mobility; Override; Trees; Modeling; Tests

1. Introduction

Both natural and rapidly emplaced man-made barriers are able either to stop or to diminish the mobility of wheeled and tracked vehicles. Understanding the override forces provides information required to assist in route planning [1]. Accurate mapping of obstacles in a real-time [2,3] environment necessitates assessing the force required to override the obstacle. When planning routes in which vertical obstacles impede forward movement, a route planner must decide whether maneuvering around or overriding the obstacles produces the optimal routing result. Part of the override decision process is based on knowing the force required to drive over the obstacle. In this study, tests were performed on vertical obstacles consisting of embedded wooden and metal posts to define override force in terms of easily observable parameters.

* Corresponding author.
E-mail addresses: George.L.Mason@us.army.mil (G.L. Mason), Burhman.Gates@us.army.mil (B.Q. Gates), Victoria.D.Moore@us.army.mil (V.D. Moore).

0022-4898/$36.00 Published by Elsevier Ltd. on behalf of ISTVS.
http://dx.doi.org/10.1016/j.jterra.2012.04.001

2. Method

Equations for vegetation override were introduced in the 1960s [5] and adapted to a mobility model [4] to support predictions for ground vehicles. The algorithms are validated for the prediction of small-diameter trees and extended for man-made obstacles such as buried fence posts.

2.1. Overriding small diameter trees

The vegetation override equations were introduced in the *NATO Reference Mobility Model* (NRMM) [4]. The NRMM is a collection of algorithms used to predict a vehicle's off-road mobility. The modeling methodology in NRMM computes individual forces acting against the forward movement of the vehicle. The vegetation override equations were derived from a series of tests conducted in the late 1960s. The equations represent forces for a vehicle's striking and/or overriding a tree of a given diameter and are determined separately from the rolling resistances of the vehicle. There are two obstacle overriding forces to

consider: an average force ($F_{average}$) and a maximum force (F_{max}). The $F_{average}$ is used to determine the required tractive effort and speed degradation during override, whereas F_{max} is used to determine whether the vehicle can override the vegetation. In certain soil conditions, it is possible that the average vegetation override force can result in immobilization. Eq. (1) defines the average force when the vehicle first engages the vegetation.

$$F_{average} = (2.62)d^3 \tag{1}$$

where d is the tree diameter in centimeters as measured at the base and F is the force in Newtons required for override.

Eq. (2) defines the maximum force required for overriding a tree given its stem diameter.

$$F_{max} = (10.86 - 0.0534h)d^3 \tag{2}$$

where h is the height in centimeters of the pushbar or forward-most part of the vehicle striking the vegetation.

From a vehicle standpoint, maximum force determines the initial change in vehicle speed by the initial shock of striking an obstacle. The total resisting force is $F_{average}$ added to other external resistances such as slope to determine the overall change in speed.

Fig. 1 illustrates results from 17 tests conducted as a part of this recent study on trees varying from 2.54 cm (1 in.) in diameter to 12.7 cm (5 in.) in diameter. The data is overlaid on test data obtained from Blackmon and Randolph [5]. Past data collection methods for vegetation override included mounting stress gauges on the front bumper of the test vehicle. A more rapid method, utilizing a cable attached to the test tree, was introduced, and the force required to fail the tree was recorded. As illustrated in Fig. 1, the data from the two independent studies appear to validate the above equations and introduce a cost-effective means of obtaining similar results. Assuming a 50.8-cm (20-in.) pushbar height, Eq. (2) is overlaid on the data. In general, with the exception of one outlier, the fit from Eq. (2) supports the relationship between tree diameter, pushbar height, and override force with a correlation of 0.78 between predicted and measured values.

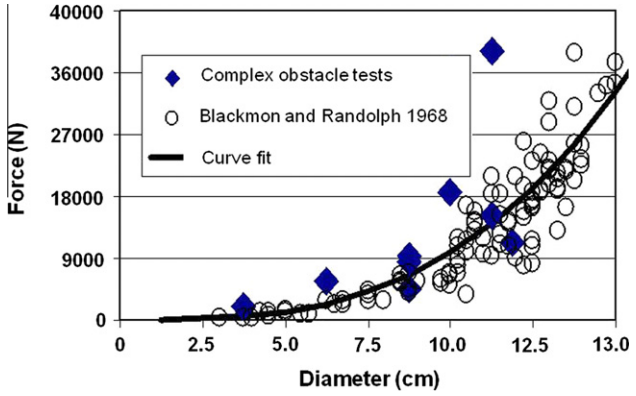

Fig. 1. Diameter of obstacle (tree) versus override force.

2.2. Overriding posts

Equations are introduced for predicting the force required to override a wooden or metal buried post. The equations are derived from summing moments about a center of rotation for the posts. As shown in Fig. 2, the distance to the center of rotation (L_p) was derived from the burial depth (L_t) and height (h) at which the extraction force (F_P) was applied. The opposing force of the soil is defined by (F_1) and (F_2) in Fig. 2 along with the distance of the aggregate forces to the center of rotation of the post in the ground (L_1) and (L_2).

The summation of moments is described in the following equation:

$$L_1F_1 + L_2F_2 - L_pF_p = 0 \tag{3}$$

The resisting force is due to the confining pressure around the post and is a function of the density of the soil and the volume of soil displaced [6]. Eq. (4) defines the maximum override force (F_p) as a function of depth of burial (L), post diameter (D), pushbar height above the center of rotation (L_p), and the dry density of the soil (γ_d).

$$\gamma_d DL_1 + \gamma_d DL_2 - L_pF_p = 0 \tag{4}$$

Eq. (5) simply isolates the term for force to override by rearranging terms from Eq. (4) and expressing L_p in terms of depth of burial (L_t) and height of pushbar above the ground (h).

$$F_p = \frac{\gamma_d D(L_1 + L_2)}{\left(h + \frac{L_t}{2}\right)} \tag{5}$$

Eq. (6) illustrates the relationship between the different moment arms as defined in Eq. (3).

$$L_1 = L_2 = \frac{L_t}{2} * \frac{2}{3} = \frac{L_t}{3} \tag{6}$$

Therefore Eq. (5) can be rewritten in terms of the total depth the post is buried (L_t) and D, h, γ_d, and a coefficient α as Eq. (7). The coefficient α is a regression coefficient correcting for unknowns in shear forces of the soil.

$$F_p = \frac{\gamma_d D\left(\frac{L_t}{3} + \frac{L_t}{3}\right)}{\left(h + \frac{L_t}{2}\right)} = \alpha\left[\frac{2}{3}\frac{\gamma_d DL_t}{\left(h + \frac{L_t}{2}\right)}\right] \tag{7}$$

3. Validation data for posts

3.1. Posts placed in indigenous material

Fence posts are often placed in the ground using one of two methods to backfill the posthole. The first method is to place the posts and to backfill rapidly with compacted material obtained from the excavation. The second method is to place the post and to backfill with concrete to increase the effective diameter of the post. The metal and wood posts for this test were buried in lean clay soil to depths of 0.305, 0.610, and 0.914 m (1–3 ft) with and without concrete backfill, as shown in Fig. 3. Weather conditions prior

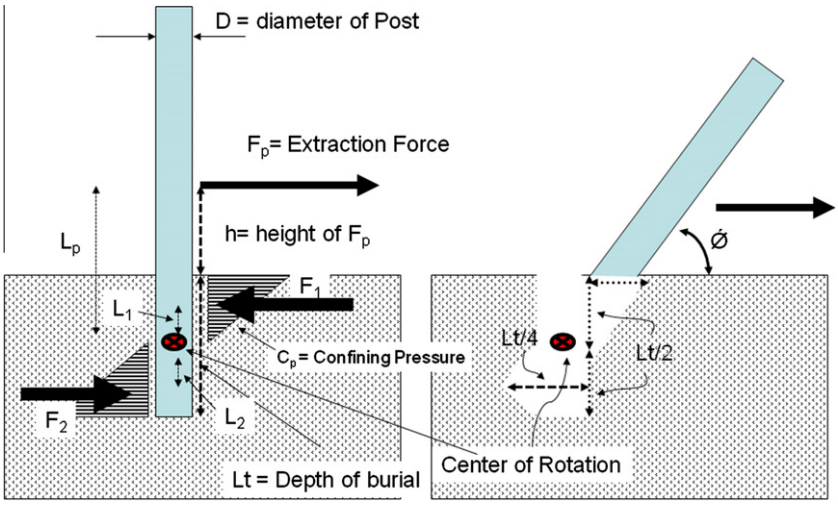

Fig. 2. Force diagram for posts.

to the tests included intermittent rainfall, which resulted in wet soil conditions. The bulk density of the soil was approximately 15710 N/m^3 (100 lb/ft^3). The lean clay soil exhibited moisture content variations between 17% and 24% with moisture content increasing slightly with depth.

Data collected at the site included the load required to pull the posts down and the total distance from the time the load was initiated until the post was completely extracted. The average distance to pull each post out of the ground was approximately 76 cm (30 in.). A load vehicle was attached to each post and/or tree at heights of 30 cm and 60 cm above the ground by way of a 11,300 N (50,000 lb) load cell and cable. A cable extension transducer (string pot) was used to measure the distance travelled by the load vehicle between the initiation of loading and failure of the post. Fig. 4 illustrates load and distance data collected while a post was pulled at 30 cm pushbar height. The data in Fig. 4 represent a 15-cm (6-in.) diameter wood post buried at 60 cm (24 in.). The change in the horizontal distance from the vehicle to the post or displacement during the failing and overturning of the post is

Fig. 3. Test posts.

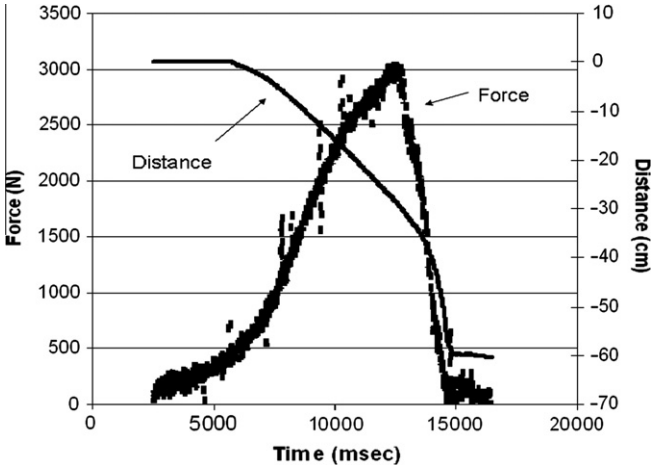

Fig. 4. Data from pull tests.

shown on the right axis in Fig. 4, starting at 0 and progressing to 60 cm (23.6 in.). The load is shown on the left axis. The load starts at zero, peaks at more than 3000 N (676 lbs), and then drops to 0. The peak or maximum load for each test was defined as the force required for overturning (i.e., overriding) the obstacle.

Tests were repeated four times for each post. Observations indicated a pattern of failure, with soil compression occurring as the post pivoted about a point half the depth of burial, as illustrated in Fig. 2. Fig. 5 illustrates a post after failure.

Fig. 6 summarizes the results for diameter, burial depth, and maximum force required to overturn posts at a 30-cm pushbar height. The horizontal distance required for pulling each post out of the ground varied from 46 cm (18 in.) to 79 cm (31 in.) with an average of 74 cm (29 in.) and a standard deviation of 8 cm (3 in.). An analysis of variance suggested there is a 95% probability that the forces required to override a wood versus a metal post are statistically different. The average increase in force from wood

Fig. 5. Posts after failure.

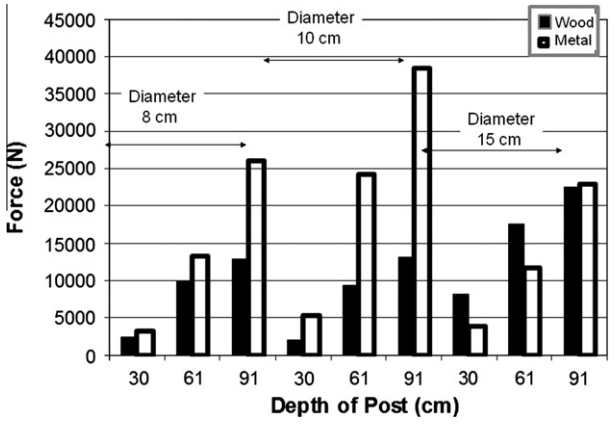

Fig. 6. Forces required to fail posts at 30-cm pushbar height.

posts to metal posts is 115%. The percent increase in force reduces at shallower depths. General observations suggested that the heavier metal posts required higher initial forces to initiate movement. These differences appeared less significant as indicated in Fig. 6 when the posts were 15 cm in diameter.

Fig. 7 summarizes the results for metal and wood posts for burial depth, diameter, and pushbar force when the height of the pushbar is 60 cm. As suggested in Eqs. (3)–(7), the forces for a 60-cm pushbar height are significantly less than those for a 30-cm pushbar height, with the amount of force required to fail the posts increasing as a function of diameter and depth of burial.

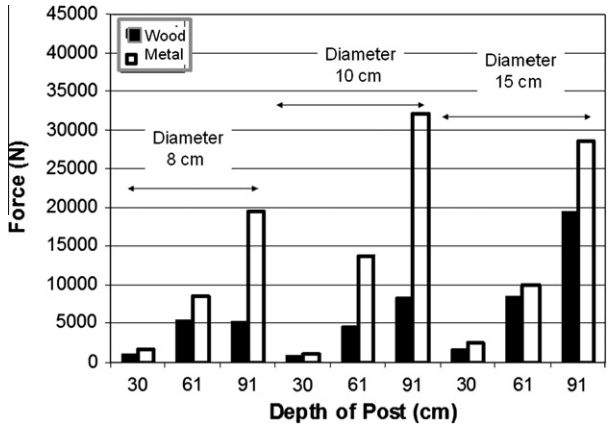

Fig. 7. Comparison of forces required to fail posts at a 60-cm pushbar height.

3.2. Posts placed in concrete footing

Holes were excavated to a diameter of 25.4 cm (10 in.), and a post was placed in each. Each hole was then filled with concrete. The equation for posts, both wood and metal, anchored in concrete was created with equating D in Eq. (5) to 25.4 cm (10 in.).

Predicted versus measured force for override is plotted in Fig. 8. A weighted least squares function was used to fit the coefficient alpha in Eq. (7) and to calculate the predicted value. The predictions were split for an alpha value of 55,000 for metal posts with a correlation coefficient of 0.69 and an alpha value of 30,000 for wood posts with a correlation coefficient of 0.92.

4. Calculation of energy required to displace posts

The previous equations were based on assuming a low constant velocity of the vehicle; introducing velocity as an additional variable requires defining the total energy expended when failing the tree or post. The energy required to fail the posts was calculated from the area under the force-versus-distance graph for 16 posts buried at different depths. Eq. (8) provides a correlation of 0.96 between maximum pulling force and energy required for the post to fail. Fig. 9 illustrates a linear relationship between the maximum pulling force and the energy absorbed by the soil.

$$E = kF_P \tag{8}$$

where E is the total energy absorbed by the soil

$k = 0.527$ m (20.74 in.), an empirical constant dependent on the soil type.

Substituting Eq. (8) into the energy equation, $E = 0.5\,mv^2$, gives the vehicle velocity, v, required at impact to

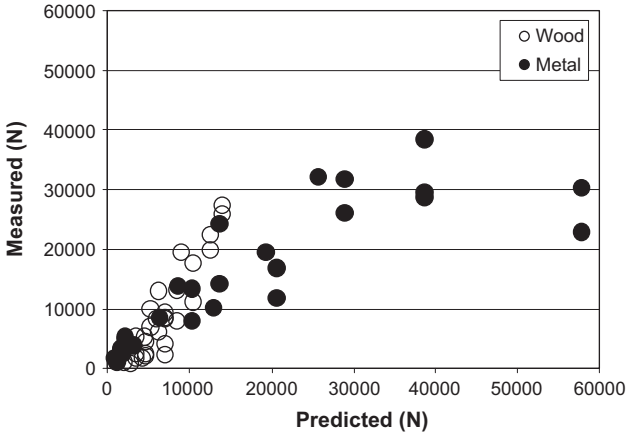

Fig. 8. Comparison of predicted versus measured force for all tests conducted on posts.

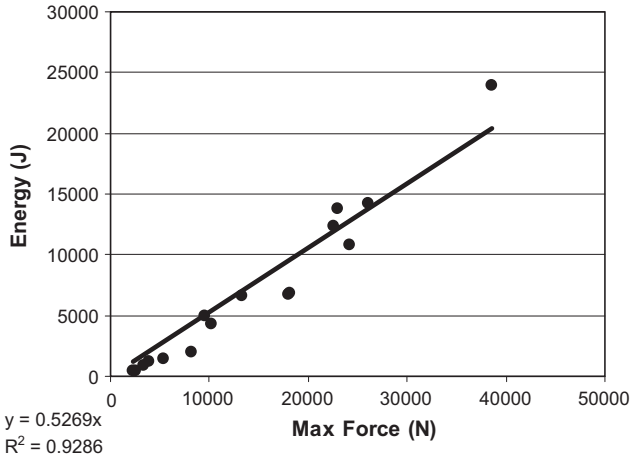

Fig. 9. Relationship between maximum force and energy (J).

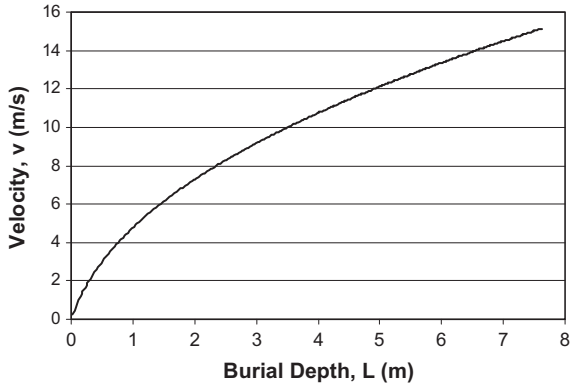

Fig. 10. Relationship between embedment depth of post and velocity to override.

fail the posts in terms of the maximum overturning resistance force, F_P, and the vehicle mass, m, as shown in Eq. (9).

$$v = \sqrt{\frac{2kF_P}{m}} \tag{9}$$

Finally, we derive Eq. (10) by substituting F_p in Eq. (9) with the relationship in Eq. (8). Eq. (10) gives the minimum vehicle velocity necessary to override the post in terms of the maximum pressure exerted by the soil, the diameter of the post, the pushbar height, and the burial depth.

$$v = \sqrt{\frac{2k\alpha\gamma_d DL_t}{m(h+\frac{L_t}{2})}} \tag{10}$$

This equation is fundamental in order to understand the effect of the post and soil parameters and their potential in vehicle-stopping capabilities. Fig. 10 shows a plot of the vehicle velocity versus the burial depth of the post for a 1362-kg (3000-lb) vehicle with a 10.16-cm (4-in.) diameter post at a pushbar height of 38.1 cm (15 in.).

5. Conclusions

This research was performed as part of ongoing ground vehicle mobility research at the Engineer Research and Development Center, and extends studies such as that of Richmond et. al. [7] in characterizing mobility performance required for unmanned ground vehicles to negotiate obstacles.

The average and maximum forces required to override a tree are given by Eqs. (1) and (2) from the NRMM. In this study, 2.54- to 12.7-cm-diameter trees were used to conduct tests to verify and validate the equations. These forces were measured and predicted independently from other forces such as rolling resistances of the tire.

The force necessary to override a post is given by Eq. (5). According to Eq. (5), a larger post diameter and a deeper burial depth will require a larger force to override the post. Similarly, the greater the pushbar height relative to the burial depth, the lower the required force will be to override the post. This pushbar-height effect is also demonstrated in Eq. (2) for trees.

The failure path demonstrated on the buried posts during testing suggests that failure starts at the soil surface, where the soil is pushed upwards by the pressure caused by the post. This result agrees with our model, where the maximum soil pressure appears at the surface.

Data suggest that the force required to override a metal post can be as much as 115% greater than that required to override a wooden post. At shallower burial depths, the percent difference in force decreases.

A linear relationship exists between the energy absorbed by the soil and the maximum pulling force, which depends on the parameter k, where k is a function of the soil type. In this study, only one soil type was considered. Future studies will be required to create parameter functions for a larger variety of soil classes. Eq. (10) provides an override velocity as a function of vehicle mass, soil parameters, the pushbar height, and post parameters (specifically the burial depth, the post material, and the post diameter or effective diameter if the post is encased in concrete.) This equation provides a better understanding of post selection and grounding and its effect on the type of vehicle it can stop or alternatively the force required to override the post as an obstacle.

Acknowledgements

The tests described and the resulting data presented herein, unless otherwise noted, were obtained from research conducted by the US Army Corps of Engineers by the Engineer Research and Development Center. Permission was granted by the Director, Geotechnical and Structures Laboratory to publish this information.

References

[1] Cummins CL, Jones RA, Gates Jr BQ. Application of an off-road mobility model to autonomous cross-country routing of unmanned ground vehicles. Unmanned Syst Technol VIII, Proc SPIE 2006;6230:623–9.

[2] Kweon IS, Kanade T. High-resolution terrain map from multiple sensor data. IEEE Trans Pattern Anal Machine Intell 1992;14(2):278–92.

[3] Henriksen L, Krotkov E. Natural terrain hazard detection with a laser rangefinder. In: Proceedings of the IEEE international conference on robotics and automation, vol. 2; 1997. p. 968–73.

[4] Ahlvin RB, Haley PW. NATO reference mobility model. 2nd ed. NRMM II User's Guide. TR GL-92-19. US Army Engineer Waterways Experiment Station, Vicksburg, MS; 1992.
[5] Blackmon CA, Randolph DD. An analytical model for predicting cross-country vehicle performance, vol. II: longitudinal obstacles. Appendix B: vehicle performance in lateral and longitudinal obstacles (vegetation). TR No. 3-783. US Army Engineer Waterways Experiment Station, Vicksburg, MS; 1968.
[6] Patzner GS. Effect of wood post strength and soil strength on the performance of the modified eccentric loader breakaway cable terminal (MELT) under impact conditions. NCHRP Report 350, Test 3-35. Master's thesis, University of Iowa; 1997.
[7] Richmond PW, Mason GL, Moore VD, Coutermarsh BA, Pusely J. Mobility performance algorithms for small unmanned ground vehicle. TR-09-6. US Army Engineer Waterways Experiment Station, Vicksburg, MS; 2009.